Investigation of the photoluminescence-linewidth broadening in periodic multiple narrow asymmetric coupled quantum wells

J. V. D. Veliadis and J. B. Khurgin
Department of Electrical and Computer Engineering, Johns Hopkins University, Baltimore, Maryland 21218

Y. J. Ding and A. G. Cui
Department of Physics and Astronomy and Center for Photochemical Sciences, Bowling Green State University, Bowling Green, Ohio 43403

D. S. Katzer
Naval Research Laboratories, Washington, D.C. 20375

(Received 17 September 1993; revised manuscript received 7 March 1994)

Photoluminescence spectra were measured as a function of temperature and excitation intensity in two periodic multiple narrow asymmetric coupled quantum-well structures. The peaks of the spectra have been identified and the temperature-dependent natures of the recombination processes have been determined. The half-widths at half maximum of the line shapes were deduced by fitting the low-energy sides to Gaussian functions. The excellent fits indicate that inhomogeneous broadening is dominant. The rate at which the linewidth broadens with temperature is more dramatic below 140 K due to the sharp changes of the ionized impurity and of the longitudinal-optical-phonon scattering mechanisms. Above 140 K, the linewidth has a linear dependence on temperature due to the thermal excitation of the longitudinal optical phonons. By using the model proposed by Lee *et al.* we have determined the scattering rates of the longitudinal acoustic and optical phonons, of the impurities, and of the inhomogeneous broadening. Our results show that unless the growth is interrupted at each interface, the inhomogeneous broadening remains dominant up to room temperature. Measurement of the temperature dependence of the photoluminescence linewidth proves to be a simple and effective technique to investigate the scattering mechanisms of the photogenerated carriers and the origins of the emission peak's linewidth broadening in these structures.

I. INTRODUCTION

The linewidth of the absorption or photoluminescence (PL) peak is very important from the viewpoints of fundamental physics and optoelectronic devices. It can be used to extract the values of carrier-scattering parameters in semiconductors, such as longitudinal-acoustic and -optical-phonon scatterings. Fluctuations of the quantum well (QW) and barrier widths from well to well or from island to island within one unit, as well as impurity effects can also be extracted from the analysis of the linewidth of the line shape. Therefore, the linewidth can be used to characterize the structural quality of the interfaces.

From a device viewpoint, the linewidth has a direct effect on the performance. The saturation intensity of the absorption peak, and the bias required to shift the transition peak in self-electro-optic-effect devices and modulators, lower as the linewidth becomes narrower. Also, a narrow PL linewidth results in more efficient QW laser devices.

Traditionally, the linewidth of the PL peak at low temperatures (a few K) has been a measure of the quality of the semiconductor material. This is because at these temperatures, broadening due to the thermal population of higher-energy levels and phonon-related effects are negligible. The narrower the linewidth, the better the quality of the material. The PL linewidth at higher temperatures, especially close to room temperature, has rarely been paid attention to. This is basically due to the presence of the numerous broadening mechanisms, which complicate the analysis of the line shape.

Recently, the PL line shape was investigated at the low temperature range of 5.4–150 K in multiple quantum wells (MQW's).[1] The experimental half-widths at half maximum (HWHM, Γ) were determined by visual inspection of the line shapes and fit to a theoretical model. At low temperatures, the low-energy sides of the line shapes overlapped with impurity-bound exciton transitions and, therefore, the HWHM had to be determined from the high-energy sides. This method cannot be applied to temperatures above 150 K, however, due to the thermal-population effect of the higher-energy levels. The spectra consist of both heavy- and light-hole peaks above 150 K, with the light-hole peak barely distinguishable as a high-energy shoulder on the heavy-hole line shape.

It is worth mentioning that the multiple transitions in the absorption and PL excitation spectra have been fit by several groups.[2,3] In order to perform accurate fitting in these cases, the band edges and binding energies of the heavy- and light-hole transitions must be calculated. Since the values of all these parameters depend on the structure, determination of the scattering rates and inho-

mogeneous broadening can be complicated. In addition, in QW laser applications the PL line shape is directly related to the lasing threshold. Thus, the PL linewidth measurement is a simpler way to investigate the scattering mechanisms and is of critical importance in the performance of modulation and laser devices based on QW's.

Multiple-narrow asymmetric-coupled quantum-well (MACQW) structures are currently being investigated for potential applications. *p-i-n* photodiodes incorporating double-narrow asymmetric-coupled quantum wells have exhibited blueshift electroabsorption.[4] Simultaneous resonant tunneling of photogenerated electrons and holes has been observed in triple-narrow asymmetric-coupled quantum wells.[5] Mid-infrared electroluminescence and lasing, associated with an intersubband transition has been observed in a narrow asymmetric-coupled-well configuration.[6] An optically pumped four-level far-infrared laser system, based on the intersubband transitions in a four-narrow asymmetric-coupled quantum-well structure (which we study here) has been proposed.[7] Although studies have been made to characterize the PL linewidth broadening in GaAs/$Al_xGa_{1-x}As$ multiple quantum wells, the effect of the narrow coupled asymmetric geometry in the PL line shape has not been investigated.

Here, we report our results[8] on the measurement of the PL spectra of two periodic MACQW samples, at temperatures in the 21–300-K range and at laser intensities in the 0.5–100-W/cm^2 range. The heavy-hole PL peaks were successfully fit by Gaussian distributions. This indicates dominant inhomogeneous broadening and allows accurate determination of the PL peak positions and of the HWHM. The HWHM were subsequently fit using a theoretical model. Above 45 K, the linewidth was determined by fitting the low-energy side of the PL peak. Hence, we were able to precisely determine the room-temperature contribution of each broadening mechanism to the line shape. This is important since most optoelectronic devices operate at room temperature. We have also demonstrated that unless the growth of the MACQW's is interrupted at each interface, inhomogeneous broadening of the PL line shapes is dominant throughout the temperature range.

II. EXPERIMENTS AND LINE-SHAPE ANALYSIS

Two MACQW samples were used in these experiments. Sample [*A*] (Fig. 1) is a 20-period GaAs/$Al_{0.4}Ga_{0.6}As$ MACQW structure, grown by molecular-beam epitaxy (MBE) on a Si-doped (100) GaAs substrate. Each period consists of four undoped GaAs quantum wells, with widths of 2, 2.5, 3.5, and 4.5 nm, coupled by undoped $Al_{0.4}Ga_{0.6}As$ barriers with widths of 3, 4, 3, and 4 nm, respectively. Sample [*B*] (Fig. 2) is a 10-period GaAs/$Al_{0.3}Ga_{0.7}As$ MACQW structure grown by MBE. Each period consists of three undoped GaAs quantum wells with widths of 5, 3, and 4.5 nm coupled by 4-nm-undoped $Al_{0.3}Ga_{0.7}As$ barriers. To obtain high-quality interfaces in sample [*B*], the MBE growth was interrupted for 60 sec at each interface. The widths of the asymmetric quantum wells in our study are about two to four times narrower than those of Refs. 1 and 2, hence the word "narrow" is used to describe them.

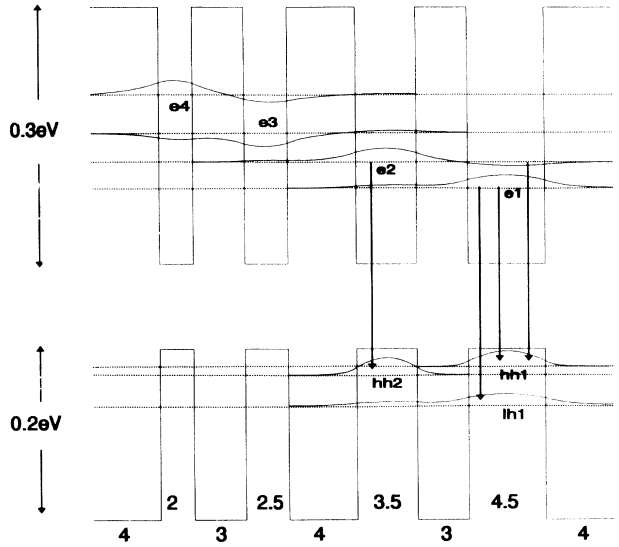

FIG. 1. One period of undoped sample [*A*] MACQW's consists of four GaAs QW's with widths of 2, 2.5, 3.5, and 4.5 nm coupled by $Al_{0.4}Ga_{0.6}As$ barriers with widths of 3, 4, 3, and 4 nm, respectively. The calculated electron and hole energy levels and wave functions are shown. Arrows, the peak transitions of the PL spectrum, see Fig. 3(a). Numbers, the well and barrier widths in nm.

The samples were mounted on the cold finger of a continuous flow, variable temperature cryostat and excited by an Ar-ion laser pumped CW dye laser. The collected PL intensity was directed into a monochromator, detected by a photomultiplier tube, and measured with a standard lock-in technique. The pump laser photon energy was fixed at $E_{\text{laser}}=1.75$ eV, well above the $E_g=1.44$ eV GaAs band gap but below the $E_g'=1.93$ and 1.79 eV bar-

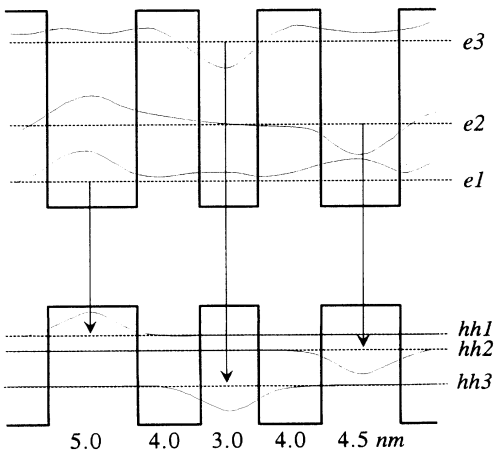

FIG. 2. One period of undoped sample [*B*] MACQW's consists of three GaAs QW's with widths of 5, 3, and 4.5 nm coupled by 4-nm $Al_{0.3}Ga_{0.7}As$ barriers. The calculated electron and hole energy levels and wave functions are shown. Arrows, the peak transitions of the PL spectrum, see Fig. 4. Numbers, the well and barrier widths.

rier energies[9] of samples [A] and [B], respectively. Typical PL spectra of sample [A] corresponding to room temperature, 175, and 78 K are presented by the dashed lines in Figs. 3(a), 3(b), and 3(c), respectively. PL spectra of sample [B] at room temperature, 215, and 185 K are presented by the dashed lines in Figs. 4(a), 4(b), and 4(c), respectively. The PL efficiency decreases by several orders of magnitude as the temperature is raised.

Based on our calculations of the energy levels in sample [A] (Fig. 1), we have identified the main peak of the PL spectrum at 773.3 nm [Fig. 3(a)] as the transition between the first electron energy level and the first heavy-hole energy level, i.e., the e_1h_1 transition of the widest well. Similarly, the first broad shoulder on the high-energy side of the main peak at 756.5 nm [Fig. 3(a)] has been identified as the band-to-band emission from the second electron energy level to the first heavy-hole energy level, e_2h_1. The second broad shoulder at 743.2 nm is the joint contribution of the e_1l_1 and e_2h_2 transitions. This assignment of the PL peaks is confirmed by the PL excitation spectra, which we measured in the 78–300 K range, as well as by our room-temperature photospectroscopic reflection measurement. At low temperatures, the thermal population of the higher electron and hole energy levels is negligible. Thus, the broad high-energy shoulders of Fig. 3(a) disappear in Figs. 3(b) and 3(c). The PL line shapes are steeper on the low-energy side down to 78 K [see Fig. 3(c)]. Similarly, based on the calculation of the energy levels (Fig. 2) and the PL excitation spectra of sample [B], the PL peaks in Figs. 4(a), 4(b), and 4(c) correspond to the e_1h_1 and e_2h_2 transitions.

The room-temperature e_1h_1 transitions are believed to occur between free carriers (not excitons) in these MACQW samples. This is justified as follows: Under CW laser pumping well above the GaAs band gap, in the steady state and at room temperature, the density of the excitons can be shown to be many orders of magnitude smaller than the density of the free carriers,[10] since the excitons at room temperature can be ionized as fast as 0.3 ps.[2,11] In the case of MACQW's, the excitons can be ionized even more rapidly due to the poor overlap between electron and hole wave functions.[4] Consistent with Refs. 12 and 13, we can therefore conclude that the room-temperature radiative recombination is taking place primarily between free carriers in MACQW's.

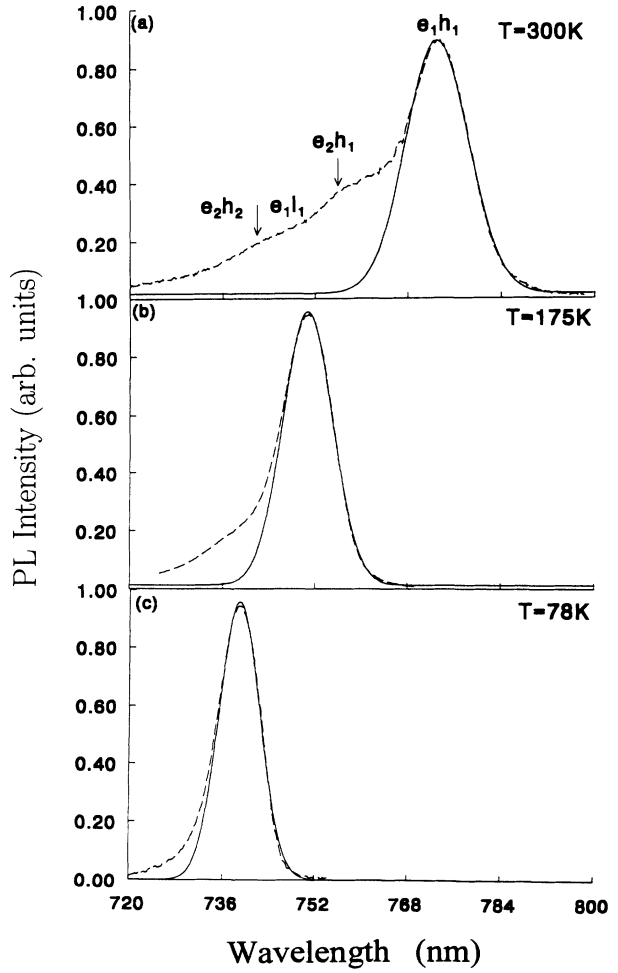

FIG. 3. Photoluminescence spectra (dashed lines) of sample [A] measured at (a) 300, (b) 175, and (c) 78 K. Arrows, the locations of the e_1h_1, e_2h_1, and the joint e_1l_1 and e_2h_2 transitions. Solid lines, Gaussian fits of the e_1h_1 transitions.

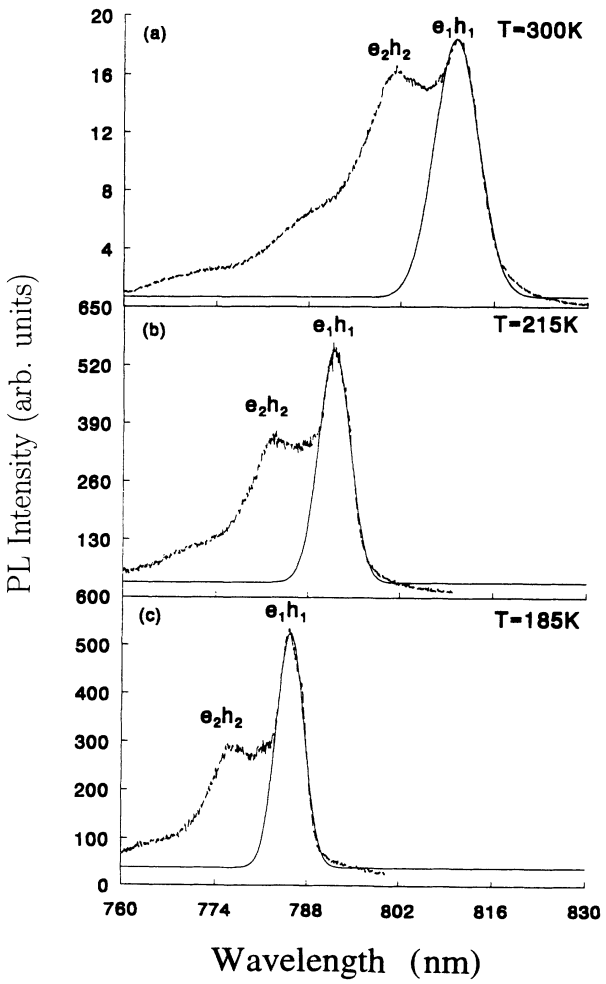

FIG. 4. Photoluminescence spectra (dashed lines) of sample [B] measured at (a) 300, (b) 215, and (c) 185 K. Solid lines. Gaussian fits of the e_1h_1 transitions.

The peak photon energies of the e_1h_1 transitions (obtained from the Gaussian fits of the 21–300-K sample [*A*] and the 78–300-K sample [*B*] PL spectra, as discussed below) are shown as a function of temperature in Fig. 5. The dashed line at lower energies is the bulk GaAs direct band gap.[9] The e_1h_1 transition energies are always higher than the band gap of bulk GaAs at the same temperature, mainly due to the quantum confinement of the electrons and holes in the MACQW's. The two solid lines in Fig. 5 have been obtained by shifting the temperature dependence of the bulk GaAs band gap, to match the e_1h_1 room-temperature transition energies. The solid line fits the experimental data of sample [*A*] very well down to 115 K. Therefore, free-carrier recombination dominates throughout the 115–300-K range. Below 115 K, however, the peak photon energies are below the shifted bulk GaAs line (Fig. 5). This energy difference ($\approx$6 meV) represents the binding energy of the e_1h_1 excitons. In the case of sample [*B*], the solid line fits the experimental e_1h_1 PL peaks fairly well throughout the 78–300-K temperature range. Free-carrier recombination is believed to take place down to 78 K.

The e_1h_1 PL peaks were fit using Gaussian distributions. This allows accurate determinations of the peak energies (used in Fig. 5) and the HWHM, Γ, of the line shapes. The excellent fitting possible, using this technique, is illustrated by the solid lines in Figs. 3 and 4. To avoid thermal effects due to the heating of the samples, the excitation intensity was fixed below 100 W/cm^2, which gives very clear PL line shapes up to 300 K. Below 45 K, the transitions from or to the impurity levels may broaden the low-PL-energy side of sample [*A*]. Thus, the high-energy sides of the e_1h_1 transitions were selected for curve fitting in this range. Above 45 K, however, the low-PL-energy sides were chosen for curve fitting in both samples. Therefore, any error due to the thermal tails of the high-energy sides is avoided and $\Gamma(T)$ is determined up to room temperature. As the temperature decreases in sample [*A*] [Figs. 3(a), 3(b), and 3(c)], the high-energy tails vanish and the PL spectra approach the Gaussian fits on the high-energy sides, too. Thus, at low temperatures, the entire line shape can be fit using a Gaussian distribution [Fig. 3(c)]. This indicates that the line shape is the result of a mainly inhomogeneously broadened[14] PL emission peak.

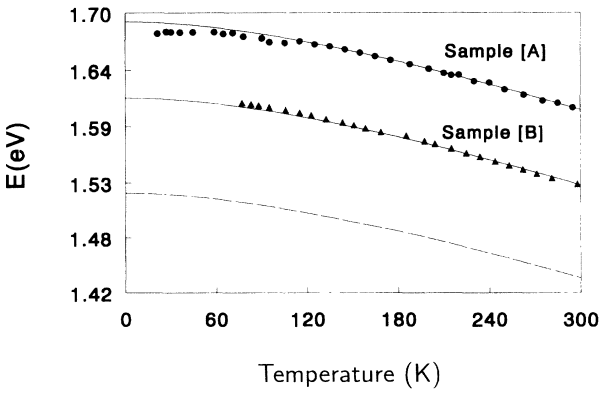

FIG. 5. Measured photon energies of the e_1h_1 peaks vs temperature for a laser intensity of 2.5 W/cm^2; filled circles, sample [*A*]; filled triangles, sample [*B*]. Dashed line, GaAs band gap vs temperature. Solid lines, GaAs band gap shifted to match the e_1h_1 room-temperature transition energies.

In agreement with previous work[1] in symmetric MQW's, we find that as the temperature is raised above 78 K, the linewidths increase monotonically. In order to interpret this type of temperature dependence, the experimental HWHM data were fit using a model[1] that includes four types of broadening mechanisms;

$$\Gamma(T)=\Gamma_0+\Gamma_{\mathrm{LA}}T+\frac{\Gamma_{\mathrm{LO}}}{[\exp(\hbar\omega_{\mathrm{LO}}/k_BT)-1]}+\Gamma_{\mathrm{imp}}\exp\left[-\frac{\langle E_B\rangle}{k_BT}\right], \quad (1)$$

where Γ_0 is the inhomogeneous broadening constant, Γ_{LA} is the longitudinal-acoustical-phonon (LA) scattering coefficient, Γ_{LO} is the longitudinal-optical-phonon (LO) scattering coefficient (with a LO phonon energy $\hbar\omega_{\mathrm{LO}}=36$ meV), and Γ_{imp} is the ionized-impurity scattering coefficient (with an average ionized-impurity binding energy $\langle E_B\rangle=5.84$ meV, Ref. 9).

The Γ coefficient values that best fit the experimental HWHM data of the two samples are presented in Table I. Equation (1) has been successfully employed in the symmetric MQW case for temperatures in the 4–150-K range. To verify that it is valid up to room temperature, the linewidth broadening study of sample [*B*] concentrates in the 169–300-K temperature range. To the best of our knowledge, this is the first study of the PL linewidth broadening mechanisms in narrow (4.5 and 5 nm) asymmetric wells at temperatures above 150 K. The experimental HWHM (filled circles), obtained as discussed above by fitting the low-energy sides of the 78–300-K sample [*A*] and the 169–300-K sample [*B*] PL spectra are presented in Figs. 6 and 7, respectively. They correspond to the linewidth broadening of the e_1h_1 transition.

The inhomogeneous broadening constant Γ_0 of sample [*A*] is significantly enhanced compared to wider symmetric MQW's and becomes the dominant broadening mechanism in this sample. It accounts for 73% of the room-temperature linewidth broadening, which is higher than any value reported[1–3] so far. The very large inhomogeneous constant in narrow wells is well accounted for

TABLE I. The scattering coefficients of the MACQW samples [*A*] and [*B*].

Sample	Γ_0 (meV)	Γ_{LA} (meV/K)	Γ_{LO} (meV)	$\Gamma_{\mathrm{imp.}}$ (meV)
[*A*]	9.59	1.45×10^{-3}	8.34	0.66
[*B*]	2.93	1.6×10^{-3}	9.58	0.85

by considering that the average well-width fluctuations[15,16] (interwell and within the layer intrawell) become more important as the layers decrease in size. Furthermore, the wells with widths of 4.5 and 3.5 nm are separated by a narrow 3-nm barrier. As a result, there is coupling of the electron-energy levels (Fig. 1) while the heavy-hole levels are more or less localized in each well. Inhomogeneous broadening is therefore enhanced in our coupled asymmetric structure because there are two adjacent wells and one barrier whose fluctuations in thickness all contribute to the PL line shape. These fluctuations (wells-barrier) have a larger effect in coupled structures like our MACQW's, similar to Ref. 4. A relatively smaller inhomogeneous broadening constant (about 8.7 meV) was reported for the 4.7-nm symmetric MQW sample of Ref. 16, where the increase of the HWHM with decreasing well size was also interpreted in terms of well-size fluctuations. As discussed above, however, in our MACQW structure, the coupling further increases the inhomogeneous broadening constant of the e_1h_1 transition. In order to reduce the large inhomogeneous broadening, the growth of sample [*B*] was interrupted for 60 sec after each epitaxial layer. This improves the interface quality of the MACQW. At the lowest PL measurement of 21 K, an inhomogeneous broadening of $\Gamma_0=2.933$ meV is determined. This corresponds to a 70% reduction compared to the Γ_0 constant of sample [*A*].

The individual contributions to the HWHM from interactions with impurities and longitudinal-optical and -acoustic phonons, superimposed above the inhomogeneous broadening line, are presented with dashed lines in Figs. 6 and 7. Below 100 K, the impurity and acoustic-phonon scattering mechanisms contribute more to the line-shape broadening than optical-phonon scattering.

The LA coefficients (Table I) $\Gamma_{LA}=1.45\times10^{-3}$ and 1.6×10^{-3} meV/K of samples [*A*] and [*B*], respectively, are in good agreement with the 1.47×10^{-3} meV/K coefficient of the wider 20-nm symmetric quantum well.[1] This agreement shows that not only does the asymmetric geometry have no noticeable effect on the LA phonon-carrier interaction, but also that the value of the LA coefficient does not depend on the width of the well.

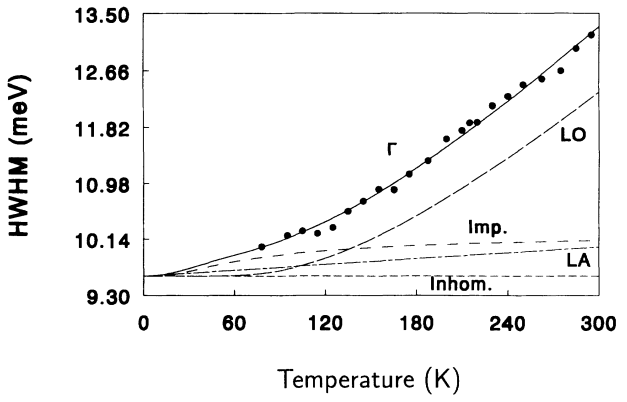

FIG. 6. Filled circles, temperature dependence of the HWHM of the e_1h_1 peaks of sample [*A*]. Solid line, the measured data are fit to Eq. (1). Dashed lines, the contributions to the HWHM from the interactions with optical phonons (LO), acoustic phonons (LA), and impurities (Imp.) superimposed above the dominant inhomogeneous broadening (Inhom.) dashed line.

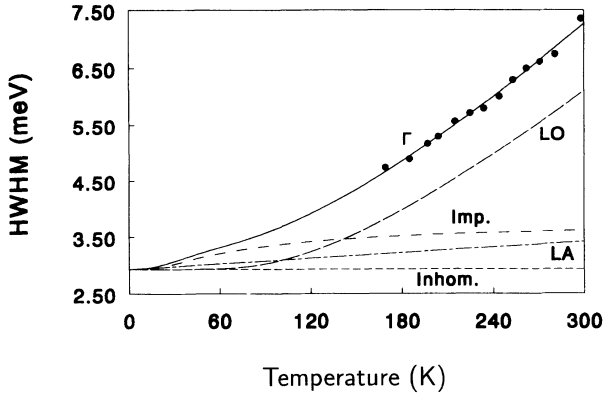

FIG. 7. Filled circles, temperature dependence of the HWHM of the e_1h_1 peaks of sample [*B*]. Solid line, the measured data are fit to Eq. (1). Dashed lines, the contributions to the HWHM from the interactions with optical phonons (LO), acoustic phonons (LA), and impurities (Imp.) superimposed above the inhomogeneous broadening (Inhom.) dashed line.

An additional broadening arises due to the scattering of the carriers by impurity donors or acceptors. The impurity coefficients (Table I) $\Gamma_{imp}=0.66$ and 0.85 meV of samples [*A*] and [*B*], respectively, are in good agreement with the 0.75-meV coefficient[1] of the 20-nm symmetric well.

The enhancement in the impurity coefficient of sample [*B*], compared to sample [*A*], is attributed to the growth interruption process that leads to increased impurity incorporation. Impurities are mainly localized at the $Al_{0.3}Ga_{0.7}As$ barriers, which are contaminated during the MBE growth. Due to the narrow geometry (Fig. 2), the first electron energy level (e_1) penetrates deeply into the adjacent barriers and therefore impurity scattering is enhanced.

The combined room temperature contribution of the LA and impurity broadenings is 7.5% in sample [*A*] and 16% in sample [*B*]. Therefore these broadening mechanisms cannot be ignored.

As the temperature increases above 140 K, scattering by longitudinal-optical phonons becomes the main temperature-dependent contributor to the line-shape broadening due to the increasing LO phonon population (Figs. 6 and 7). The LO phonon scattering terms $\Gamma_{LO}=8.34$ and 9.58 meV for samples [*A*] and [*B*], respectively, are higher than the 7-meV coefficient of bulk GaAs.[17] LO phonon scattering accounts for 21% and 44% of the room-temperature broadening in samples [*A*] and [*B*], respectively. Γ_{LO} coefficients of 4.0 (Ref. 1), 5.0 (Ref. 1), and 5.5 (Ref. 2) meV have been reported for symmetric MQW's with widths of 20, 10, and 10.2 nm, respectively. A $\Gamma_{LO}=8$ meV coefficient is approximately

the same for the four single quantum wells of Ref. 18 with widths of 3.8, 6.4, 10.1, and 14.2 nm, respectively. We conclude then, that the electron-LO phonon interaction is slightly enhanced in our narrow MACQW samples.

It is noteworthy that in sample [A], the rate of increase of $\Gamma(T)$ is more dramatic below 140 K. This is due to the sharp changes of the $\Gamma_{\text{imp}}(T)$ rate in the 78–100-K range and the $\Gamma_{\text{LO}}(T)$ rate in the 78–140-K range. Above 140 K, $\Gamma(T)$ is approximately linear in both samples, since the dominant temperature-dependent contribution $\Gamma_{\text{LO}}(T)$ approaches a linear $kT/\hbar\omega_{\text{LO}}$ dependence at higher temperatures.

By fitting the experimental HWHM data of the two MACQW structures [based on Eq. (1)], we conclude that the values of the LA and LO phonon-scattering coefficients and of the ionized impurity coefficients agree with each other within an order of magnitude. Therefore their values do not change significantly from sample to sample. The inhomogeneous constant changes drastically, however, due to the growth interruption that leads to high-quality interfaces in sample [B]. Following these discussions, we conclude that the measurement of the PL linewidth as a function of temperature, to room temperature, is a simple and effective technique to investigate the scattering mechanisms of the photogenerated carriers and the origins of the emission peak's linewidth broadening.

In our MACQW's, we have shown the existence of deep traps by measuring the dependence of the PL on the laser intensity, as in Refs. 13 and 19. The PL has a quadratic dependence on a relatively low laser intensity, and a linear dependence on a relatively high laser intensity. Since carrier trapping and nonradiative recombination determine the density of carriers, one may question whether these processes contribute to the PL line shape. By measuring the PL as a function of the laser intensity, we have concluded that the existence of deep traps does not affect the PL line shape.

III. CONCLUSION

In conclusion, we have measured the photoluminescence linewidth in the 78–300- and 169–300-K temperature ranges in two multiple-narrow asymmetric-coupled QW samples. By fitting the line shapes to Gaussian functions, we can precisely determine the half-widths at half maximum of the e_1h_1 emission peaks. The scattering rates of the carriers by the different broadening mechanisms, have been successfully determined by use of a previous theoretical model, which has given good results to room temperature. We demonstrated that unless the growth is interrupted at each interface, the inhomogeneous broadening of the line shape is dominant over the entire temperature range.

ACKNOWLEDGMENTS

This work was supported by AFOSR, NSF, and ONR. Y.J.D. is thankful to his university for providing funds for this project. We are indebted to S. J. Lee for producing Fig. 1 of this paper and to Dr. D. Wickenden of the Applied Physics Laboratory for the 21–78-K PL measurements.

[1] J. Lee, E. S. Koteles, and M. O. Vasell, Phys. Rev. B **33**, 5512 (1986).

[2] D. S. Chemla, D. A. B. Miller, P. W. Smith, A. C. Gossard, and W. Wiegmann, IEEE J. Quantum Electron. **20**, 265 (1984).

[3] H. Iwamura, H. Kobayashi, and H. Okamoto, Jpn. J. Appl. Phys. **23**, L795 (1984).

[4] Y. J. Ding, C. L. Guo, S. Li, J. B. Khurgin, K.-K. Law, J. Stellato, C. T. Law, A. E. Kaplan, and L. A. Coldren, Appl. Phys. Lett. **59**, 1025 (1991).

[5] G. W. Bryant, J. L. Bradshaw, R. P. Leavitt, M. S. Tobin, and J. T. Pham, Appl. Phys. Lett. **63**, 1357 (1993).

[6] J. Faist, F. Capasso, C. Sirtori, D. L. Sivco, A. L. Hutchinson, S. N. G. Chu, and A. Y. Cho, Electron. Lett. **29**, 2230 (1993); OSA Ann. Meet. Tech. Dig. **8**, CPD1 (1994).

[7] G. Sun and J. B. Khurgin, IEEE J. Quantum Electron. **29**, 1104 (1993).

[8] J. V. D. Veliadis, Y. J. Ding, and J. B. Khurgin, Bull. Am. Phys. Soc. **38**, 1754 (1993).

[9] G. Harbeke, O. Madelung, and U. Rössler, in *Semiconductors*, edited by K.-H. Hellwege, Landolt-Börnstein, New Series, Group III, Vol. 17, Pt. 2 (Springer-Verlag, Berlin, 1982).

[10] D. S. Chemla and D. A. B. Miller, J. Opt. Soc. Am. B **2**, 1155 (1985); S. H. Park, J. F. Morhange, A. D. Jeffery, R. A. Morgan, A. Chavez-Pirson, H. M. Gibbs, S. W. Koch, N. Peyghambarian, M. Derstine, A. C. Gossard, J. H. English, and W. Wiegmann, Appl. Phys. Lett. **52**, 1201 (1988).

[11] W. H. Knox, R. L. Fork, M. C. Downer, D. A. B. Miller, D. S. Chemla, C. V. Shank, A. C. Gossard, and W. Wiegmann, Phys. Rev. Lett. **54**, 1306 (1985).

[12] J. E. Fouquet and A. E. Siegman, Appl. Phys. Lett. **46**, 280 (1985); J. E. Fouquet, A. E. Siegman, R. D. Burham, and T. L. Paoli, *ibid.* **46**, 374 (1985); J. E. Fouquet and R. D. Burnham, IEEE J. Quantum Electron. **22**, 1799 (1986); B. Sermage, F. Alexandre, J. Beerens, and P. Tronc, Superlatt. Microstruct. **6**, 373 (1989).

[13]Y. J. Ding, C. L. Guo, J. B. Khurgin, K.-K. Law, and J. L. Merz, Appl. Phys. Lett. **60**, 2051 (1992).

[14]H. B. Bebb and E. W. Williams, in *Semiconductor Semimetals,* edited by R. K. Willardson and A. C. Beer (Academic, New York, 1972), Vol. 8, p. 290.

[15]C. Weisbuch, R. Dingle, A. C. Gossard, and W. Wiegmann, Solid State Commun. **38**, 709 (1981).

[16]L. Goldstein, Y. Horikoshi, S. Tarucha, and H. Okamoto, Jpn. J. Appl. Phys. **22**, 1489 (1983).

[17]V. I. Alperovich, V. M. Zalekin, A. F. Kranchenko, and A. S. Terekhev, Phys. Status Solidi **17**, 466 (1976).

[18]Y. J. Chen, E. S. Koteles, J. Lee, J. Y. Chi, and B. S. Elman, SPIE Quantum Well Superlatt. Phys. **792**, 162 (1987).

[19]Y. J. Ding, J. V. D. Veliadis, and J. B. Khurgin, J. Appl. Phys. **75**, 1729 (1994); J. V. D. Veliadis, Y. J. Ding, and J. B. Khurgin, to appear in J. Lum.